Thermal Conductivity of MgO Periclase from Equilibrium First Principles Molecular Dynamics

Nico de Koker*

Bayerisches Geoinstitut, University of Bayreuth, Bayreuth, Germany

A method is presented by which the lattice thermal conductivity can be computed from first principles using relatively small system sizes and simulation times. The method uses the relation for thermal conductivity of a kinetic gas, with phonon lifetimes and frequencies determined by combining equilibrium first principles molecular dynamics and first principles lattice dynamics. To illustrate the method, the lattice conductivity is computed for MgO periclase. For individual wave vectors and vibrational modes, phonon lifetimes in periclase are found to be inversely proportional to temperature, with optic modes shorter lived than acoustic modes, contributing only ~5% to the lattice conductivity. Computed thermal conductivity values show excellent agreement with experimental measurements, and suggest that the radiative contribution to thermal transport in periclase starts playing a role above ~1500 K.

Conductive transport of heat in an anisotropic material in response to a thermal gradient ∇T is described by Fourier's equation

$$\mathbf{Q} = -\mathcal{K}_{ij}\nabla T, \tag{1}$$

where $\mathbf{Q}$ is the heat flux vector and $\mathcal{K}_{ij}$ is the thermal conductivity tensor [1], which reduces to a scalar in materials where anisotropy is weak or absent. $\mathcal{K}_{ij}$ represents the combined effect of heat transport via electrons, photons, and phonons. In dielectric materials, the electronic contribution is negligible, and the radiative contribution only important at high temperatures [2], so that heat is transported primarily through lattice vibrations.

Given the technical challenges associated with the measurement of $\mathcal{K}$ at pressures in excess of 10 GPa [3–6], its theoretical computation can be of significant utility to high pressure and planetary sciences, further allowing the lattice contribution to be studied separately, directly testing the theoretical description of lattice conductivity. This may either be done though anharmonic lattice dynamics [7], or via molecular dynamics simulations. In the nonequilibrium molecular dynamics approach, conductivity is obtained through the application and maintenance of periodic thermal gradients [8–11], while in the equilibrium molecular dynamics approach conductivity is computed from either the heat flux autocorrelation [12–14], or the mean phonon lifetime [13–15]. It is this latter approach which we will pursue here.

Because finite conductivity is the result of anharmonic lattice vibrations, theoretically computed values are very sensitive to the form of the potential applied in the simulation. Empirical potentials are not sufficiently accurate, and cannot be used at high pressures where the experimental data required for their constraint is insufficient. These concerns fall away when using first principles methods, where the potential is obtained *in situ* from the relaxed charge density via density functional theory [16–18].

Unfortunately, these methods are very computationally intensive, limiting system sizes to at most a few hundred atoms.

In this study we present a method by which the effective lattice conductivity $\mathcal{K}$ can be computed using first principles molecular dynamics (FPMD). We illustrate the method with MgO periclase, a face-centered cubic oxide that has been previously investigated both experimentally and computationally. The large electronic band gap (6.5 eV [19]) assures negligible radiative and electronic contributions, and facilitates direct comparison of computed lattice conductivities to experimental measurements. The presence of optic modes further allows us to test their conductive contribution, and thus assess their importance for conduction in more complex minerals.

To the extent that anharmonicity may be viewed as a perturbation of the harmonic description, lattice conductivity occurs as heat transport by phonons. By describing the steady state spatial redistribution of the phonon population $\mathcal{N}$ under the influence of a thermal gradient ∇T, the thermal transport properties of the lattice can be derived. The Boltzmann equation describes the steady state resistance to phonon diffusion arising from scattering off grain boundaries, lattice defects, and other phonons [2,20,21],

$$\left.\frac{\partial \mathcal{N}}{\partial t}\right|_{\mathrm{diff}} + \left.\frac{\partial \mathcal{N}}{\partial t}\right|_{\mathrm{scatt}} = 0. \tag{2}$$

If the variation of the phonon distribution from the mean $\bar{\mathcal{N}}$ is small, (2) can be solved by linearizing the scattering term, introducing a mean phonon lifetime τ,

$$\left.\frac{\partial \mathcal{N}}{\partial t}\right|_{\mathrm{scatt}} = \frac{\mathcal{N} - \bar{\mathcal{N}}}{\tau}. \tag{3}$$

In essence this approximation views phonons as harmonic but of finite lifetime, i.e., as a kinetic gas of phonons interacting only by instantaneous collisions. The solution

to the Boltzmann equation for $\mathcal{K}$ in an isotropic periodic solid with n atoms per unit cell is then equivalent to that which describes the conductivity of a kinetic gas of elastic particles [2,20,21],

$$\mathcal{K} = \sum_s^{3n} \int_{\mathbf{q}} v_{\mathbf{q},s}^2 c_{\mathbf{q},s} \tau_{\mathbf{q},s} d\mathbf{q}, \qquad (4)$$

where $v_{\mathbf{q},s} = |\mathbf{v}_{\mathbf{q},s}|$ is the phonon group velocity,

$$\mathbf{v}_{\mathbf{q},s} = \frac{\partial \nu_{\mathbf{q},s}}{\partial \mathbf{q}}, \qquad (5)$$

and $c_{\mathbf{q},s}$ is the mode heat capacity,

$$c_{\mathbf{q},s} = \frac{k_B}{V} \frac{x^2 e^x}{(e^x - 1)^2}; \qquad x = \frac{h\nu_{\mathbf{q},s}}{k_B T}. \qquad (6)$$

To compute $\mathcal{K}$ via (4), relaxation times and vibrational frequencies are needed as a function of wave vector.

Consider an infinite lattice with n atoms per unit cell, not necessarily of the same chemical species. With the position, velocity, and mass of particle a of primitive cell A at time $t > 0$, respectively, denoted as $\mathbf{r}_a^A(t)$, $\mathbf{u}_a^A(t)$, and m_a, the weighted velocity field

$$\mathbf{u}(\mathbf{r}, t) = \sum_A^{\infty} \sum_a^n \sqrt{m_a}\, \mathbf{u}_a^A(t) \delta[\mathbf{r} - \mathbf{r}_a^A(t)] \qquad (7)$$

has reciprocal space representation

$$\mathbf{u}(\mathbf{q}, t) = \int_{-\infty}^{\infty} \mathbf{u}(\mathbf{r}, t) \exp(i\mathbf{q} \cdot \mathbf{r}(t)) d\mathbf{r}. \qquad (8)$$

From the velocity autocorrelation function of the lth velocity component [22],

$$J_l(\mathbf{q}, t) = \lim_{t_0 \to \infty} \frac{1}{t_0} \int_0^{t_0} u_l(\mathbf{q}, t) u_l(\mathbf{q}, t + t') dt', \qquad (9)$$

follows the spectral density by Fourier transformation,

$$g_l(\mathbf{q}, \nu) = \frac{4}{k_B T} \int_0^{\infty} J_l(\mathbf{q}, t) \exp(2\pi i \nu t) dt. \qquad (10)$$

In the phonon lifetime approximation, the velocity autocorrelation function at a specific wave vector will be a Fourier sum of $3n$ damped harmonic oscillators,

$$J_l'(\mathbf{q}, t) = J_l^0 \sum_s^{3n} \cos(2\pi \nu_{\mathbf{q},s} t) \exp(-t/\tau_{\mathbf{q},s}), \qquad (11)$$

where $J_l^0 = J_l(\mathbf{q}, 0)$. The spectral density of $J_l'(q, t)$ consists of $3n$ delta functions, each convolved with the Fourier transform of the associated exponential function describing the mode lifetime,

$$g_l'(\mathbf{q}, \nu) = \sum_s^{3n} \frac{2 J_l^0 \tau_{\mathbf{q},s}}{1 + (2\pi \tau_{\mathbf{q},s}(\nu - \nu_{\mathbf{q},s}))^2}. \qquad (12)$$

To the extent that the phonon lifetime approximation is

accurate, $g_l(\mathbf{q}, \nu) = g_l'(\mathbf{q}, \nu)$ is valid and the lifetime can be obtained from the atomic phase trajectories.

In practice we have access only to systems of finite duration and size, and $J_l(\mathbf{q}, t)$ has to be damped to zero for Fourier transformation to be performed. The damping function is chosen such that its convolution with the spectral peaks can be analytically accounted for in the width of the spectral peak. An exponential function (decay time τ_{damp}) is ideal for this, so that τ follows from the width of the spectral peak τ_{peak} as

$$1/\tau = 1/\tau_{\text{peak}} - 1/\tau_{\text{damp}}. \qquad (13)$$

We compute $J_l(\mathbf{q}, t)$ using FPMD at the accessible exact wave vectors (a consequence of the finite system size), and obtain vibrational frequencies over the entire Brillouin zone using first principles lattice dynamics (FPLD). To the extent that they agree with frequencies obtained from $g_l(\mathbf{q}, \nu)$, these harmonic frequencies give accurate values for $\mathbf{v}_{\mathbf{q},s}$ and $c_{\mathbf{q},s}$.

Thermodynamic properties of MgO periclase were previously computed using FPMD in the NVT ensemble, in excellent agreement with the available thermodynamic and shock compression data to very high pressures (260 GPa) [23]. Details of the FPMD method are discussed in previous studies [23,24]. First principles calculations are performed using VASP [25], combined with PHONON [26] to compute phonon spectra. Exchange and correlation effects are evaluated via the local density approximation (LDA), with electronic wave functions represented with ultrasoft pseudopotentials [27].

Five FPMD simulations were performed using a $2 \times 2 \times 2$ supercell of eight fcc unit cells (64 atoms) [28] in the NVE ensemble [29] at the LDA relaxed volume, with resulting mean pressures and temperatures of $[P(\text{GPa}), T(\text{K})] = [6.56, 680]$ [9.78, 1180], [11.99, 1530], [14.04, 1860], and [17.16, 2350]. The increase in pressure with temperature arises due to thermal expansivity, another expression of anharmonicity. To evaluate finite size effects, a $3 \times 3 \times 3$ supercell simulation was also performed (216 atoms; $[P, T] = [8.18, 957]$). NVE simulations are initiated using the electronic charge density, atomic positions and velocities from NVT simulations equilibrated at the desired temperature over at least 4000 time steps (femtoseconds). Each NVE simulation is run for a total of 40 000 time steps, with the first 10 000 steps allowing for equilibration of vibrational modes. The force constant matrix was computed using a $4 \times 2 \times 2$ supercell [30], with the dielectric constant and effective charges obtained from the literature (3.10 and ± 1.93 [31]).

Phonon spectra determined from the force constant matrix are in excellent agreement with experimental data [32] as well as with a previous FPLD study [31]. Vibrational frequencies obtained from the phase trajectories are very similar to the harmonic values (Fig. 1), so that group velocities determined from harmonic frequencies are suf-
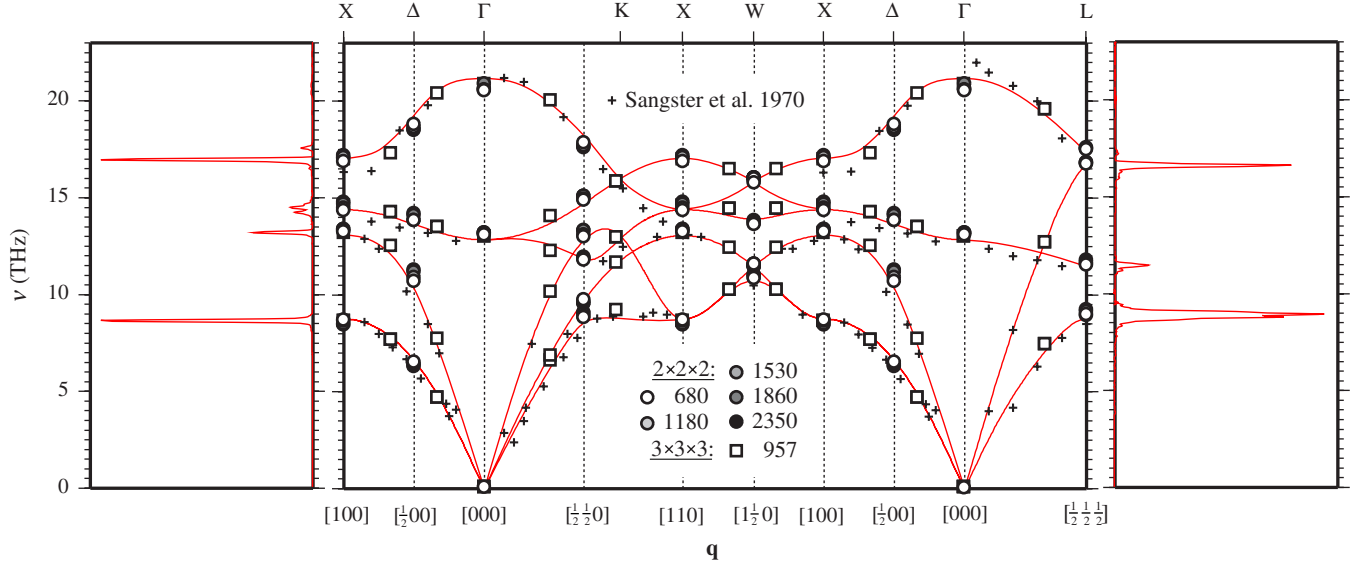
FIG. 1 (color online).   (middle) Anharmonic phonon frequencies from FPMD at exact wave vectors (circles—64 atom cell, squares—216 atom cell; T values in K) compared with harmonic frequencies calculated from the force constant matrix (solid lines). Temperature dependence of anharmonic frequencies is in general small enough that $\mathbf{v}_{\mathbf{q},s}$ and $c_{\mathbf{q},s}$ can be accurately computed from harmonic frequencies. Crosses are inelastic neutron scattering data of Sangster *et al.* [32]. (left and right panels) Examples of FPMD spectral peaks, at [100] and $[\frac{1}{2}\frac{1}{2}\frac{1}{2}]$, from which phonon lifetimes are determined.

ficiently accurate to compute the group velocities and modal heat capacities.

Phonon lifetimes at individual wave vectors and vibrational modes are found to decrease with temperature, consistent with proportionality $1/\tau_{\mathbf{q},s} \propto T$ (Fig. S1 of [33]). Indeed, for simple compounds the phonon lifetime is theoretically expected to vary as [21]

$$1/\tau_{\mathbf{q},s} = \mathcal{A}_{\mathbf{q},s} T \nu^2, \qquad (14)$$

where $\mathcal{A}_{\mathbf{q},s}$ are proportionality constants. For MgO we find $\mathcal{A}_{\mathbf{q},s}$ to show notable anisotropy in MgO, but because $\mathcal{K}$ is an integration of $\tau_{\mathbf{q},s}$ values over the Brillouin zone (4), mean values ($\bar{\mathcal{A}}_s$) for each mode may be used to evaluate $\mathcal{K}$.

The lattice conductivity for periclase computed using (4) is shown in Fig. 2, together with the value computed using the larger supercell, and previous experimental and theoretical determinations. Agreement between the computation and experimental values is excellent, although direct comparison is possible only between 500–1200 K, where theoretical pressures are comparable to those at which experimental measurements are available [3]. Comparison to higher temperature experimental values suggests that the radiative conductivity is significant above ~1500 K.

Group velocity values for optic modes are notably smaller than for acoustic modes (Fig. 1). For a homogeneous phonon lifetime, optic modes contribute 6.7% to the total lattice conductivity. However, because computed optic phonon lifetimes are somewhat smaller than for acoustic modes, this contribution reduces to 4.9% in periclase. Indeed, studies employing the kinetic conductivity equa-

tion often assume contributions from optic modes to be negligible [34,35], although the extent to which this approximation holds for more complex structured minerals remains to be tested.

One possible concern for computational accuracy is the effect of the relatively small simulation cell on $\bar{\mathcal{A}}_s$ and $\tau_{\mathbf{q},s}$ itself. Although a larger sampling of the Brillouin zone will yield a more representative averaging for $\bar{\mathcal{A}}_s$, comparison of $\mathcal{A}_{\mathbf{q},s}$ values at [100] to $[\frac{1}{2}00]$, and at $[\frac{1}{2}\frac{1}{2}0]$ to $[1\frac{1}{2}0]$ indicates that τ varies primarily as a function of azimuth, and less so radially (Fig. S1 of [33]). It is therefore unlikely that $\bar{\mathcal{A}}_s$ determined from a larger set of $\mathbf{q}$ points would vary by more than $\pm 1\sigma$ from the mean $\bar{\mathcal{A}}_s$ values. Comparison of $\bar{\mathcal{A}}_s$ for the 64 and 216 atom systems shows this indeed to be the case, while the $\tau_{\mathbf{q},s}$ values for the shared wave vectors (Γ and X) are robust to within the uncertainty of individual $\mathcal{A}_{\mathbf{q},s}$ fits (Fig. S1 of [33]). This suggests that $\tau_{\mathbf{q},s}$ is not very sensitive to system size, so that the method presented can yield accurate effective $\mathcal{K}$ values, from first principles, using relatively few atoms.

To summarize, an new method to compute lattice thermal conductivity in crystalline solids has been introduced which is accurate as well as computationally efficient. The method is based on the kinetic conductivity relation, with phonon lifetimes, group velocities, and heat capacities obtained by combining first principles molecular dynamics and lattice dynamics. Lattice conductivity for MgO periclase has been computed, and is in excellent agreement with the available experimental data, also resolving the relative conductive contributions from individual modes. The use of first principles calculations renders the method
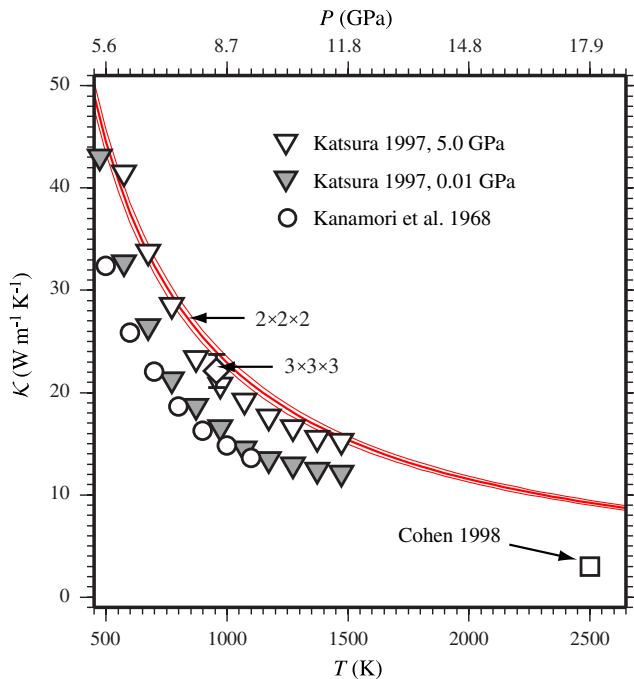
FIG. 2 (color online). Thermal conductivity of MgO at the LDA relaxed volume ($V = 10.998$ cm^3 mol^{-1}). Thick line with uncertainty envelope—64 atom cell; diamond—216 atom cell. Pressures to which various temperatures correspond are indicated on the top axis, and include a correction for LDA overbinding [23,24]. Previous work: Katsura [3], Kanamori *et al.* [36], Cohen [12].

predictive, and thus ideal for constraining lattice conductivity at extreme physical conditions.

---

*nico.dekoker@uni-bayreuth.de

 [1] J. F. Nye, *Physical Properties of Crystals* (Oxford University Press, Oxford, 1957), 1st ed.
 [2] J. M. Ziman, *Electrons and Phonons* (Oxford University Press, Oxford, 1960).
 [3] T. Katsura, Phys. Earth Planet. Inter. **101**, 73 (1997).
 [4] M. Manga and R. Jeanloz, J. Geophys. Res. **102**, 2999 (1997).
 [5] Y. Xu, T. J. Shankland, S. Linhardt, D. C. Rubie, F. Langenhorst, and K. Klasinksi, Phys. Earth Planet. Inter. **143–144**, 321 (2004).

 [6] P. Beck, A. F. Goncharov, V. V. Struzhkin, B. Militzer, H.-K. Mao, and R. J. Hemley, Appl. Phys. Lett. **91**, 181914 (2007).
 [7] D. A. Broido, M. Malorny, G. Birner, N. Mingo, and D. A. Steward, Appl. Phys. Lett. **91**, 231922 (2007).
 [8] D. J. Evans, Phys. Lett. A **91**, 457 (1982).
 [9] F. Müller-Plathe, J. Chem. Phys. **106**, 6082 (1997).
[10] P. Jund and R. Julien, Phys. Rev. B **59**, 13 707 (1999).
[11] S. Stackhouse, L. Stixrude, and B. B. Karki, Eos Trans. AGU 89, Fall M. Supp., Abs. MR21C (2008).
[12] R. Cohen, Rev. High Pres. Sci. Tech. **7**, 160 (1998).
[13] S. Volz, J. B. Saulnier, M. Lallemand, B. Perrin, P. Depondt, and M. Mareschal, Phys. Rev. B **54**, 340 (1996).
[14] A. J. H. McGaughey and M. Kaviany, Phys. Rev. B **69**, 094303 (2004).
[15] H. Zhao and J. B. Freund, J. Appl. Phys. **104**, 033514 (2008).
[16] P. Hohenberg and W. Kohn, Phys. Rev. **136**, B864 (1964).
[17] W. Kohn and L. J. Sham, Phys. Rev. **140**, A1133 (1965).
[18] N. D. Mermin, Phys. Rev. **137**, A1441 (1965).
[19] S. P. Kowalczyk, F. R. McFeely, L. Ley, V. T. Gritsyna, and D. A. Shirley, Solid State Commun. **23**, 161 (1977).
[20] R. Peierls, Ann. Phys. (Leipzig) **395**, 1055 (1929).
[21] P. G. Klemens, in *Solid State Phys.*, edited by F. Seitz and D. Turnbull (Academic Press Inc., New York, 1958), Vol. 7, pp. 1–98.
[22] D. A. McQuarrie, *Statistical Mechanics* (University Science Books, Sausalito, CA, 1984).
[23] N. de Koker and L. Stixrude, Geophys. J. Int. **178**, 162 (2009).
[24] N. de Koker, L. Stixrude, and B. B. Karki, Geochim. Cosmochim. Acta **72**, 1427 (2008).
[25] G. Kresse and J. Furthmüller, Comput. Mater. Sci. **6**, 15 (1996).
[26] K. Parlinski, computer code PHONON, Cracow, 2008.
[27] G. Kresse and J. Hafner, J. Phys. Condens. Matter **6**, 8245 (1994).
[28] For this particular supercell, exact wave vectors are at [i/l, j/l, k/l], where $l = 2$ and $i, j, k \in$ integers.
[29] Thermostats applied in *NVT* MD introduce additional scattering of phonons [D. Frenkel and B. Smit, *Understanding Molecular Simulation: From Algorithms to Applications* (Academic Press, San Diego, 1996), 1st ed.].
[30] Force constants were found to be converged for a $4 \times 8 \times 8$ k-point mesh and 600 eV basis set cutoff energy.
[31] B. B. Karki, R. M. Wentzcovitch, S. De Gironcoli, and S. Baroni, Phys. Rev. B **61**, 8793 (2000).
[32] M. J. L. Sangster, G. Peckham, and D. H. Saunderson, J. Phys. C **3**, 1026 (1970).
[33] See EPAPS Document No. E-PRLTAO-103-019941 for a supplemental figure. For more information on EPAPS, see http://www.aip.org/pubservs/epaps.html.
[34] G. A. Slack, in *Solid State Physics*, edited by H. Ehrenreich, F. Seitz, and D. Turnbull (Academic Press, Inc., New York, 1979), Vol. 34, pp. 1–71.
[35] A. M. Hofmeister, Science **283**, 1699 (1999).
[36] H. Kanamori, N. Fujii, and H. Mizutani, J. Geophys. Res. **73**, 595 (1968).